Structural features of the intermetallic compounds Pr_2M_{17} (M=Fe, Co) and implications on magnetic properties

G. Calestani,[1] N. Magnani,[2,3] A. Paoluzi,[2] L. Pareti,[2] and C. Rizzoli[1]
[1]*Dipartimento di Chimica GIAF, Università di Parma, Parco Area delle Scienze 17/A, I-43100 Parma, Italy*
[2]*IMEM, Consiglio Nazionale delle Ricerche, Parco Area delle Scienze 37/A, I-43100 Parma, Italy*
[3]*INFM and Dipartimento di Fisica, Università di Parma, Parco Area delle Scienze 7/A, I-43100 Parma, Italy*
(Received 4 April 2003; published 26 August 2003)

Novel structural features have been shown by single-crystal x-ray diffraction (XRD) in Pr_2Fe_{17} and Pr_2Co_{17} intermetallic compounds. Some of these features are common characteristics of the two compounds, while others appear to be specific to the cobalt- or iron-based phase. It has been found that in both cases the suitable space group for the description of the rhombohedral Pr_2M_{17} (M=Fe, Co) structure is $R3m$ and not the usually considered centrosymmetric $R\bar{3}m$ group. This results in a puckered arrangement of the M atoms in the $3d$-metal plane and in the nonsymmetric position of the two crystallographically independent Pr atoms with respect to the $3d$ metal atoms in the mixed Pr-M layer. The Pr-Fe compounds are always stoichiometric even in the presence of excess Pr in the starting nominal composition. The real structure is characterized by a very frequent occurrence of obverse-reverse twinning domains stacked along the c axis. The presence of multiple Pr sites and, as a consequence, of different contributions to the magnetocrystalline anisotropy is the key to explaining the occurrence of a double field-induced transition in the magnetization curve of Pr_2Fe_{17} compounds. In contrast some excess Pr was found in the cobalt compounds. Two groups of samples having, respectively, low ($\simeq$1%) and high ($\simeq$5%) excess Pr and consequently different anisotropy field values were found, depending on the starting nominal composition. The origin of the differences observed in Fe and Co compounds is discussed.

DOI: 10.1103/PhysRevB.68.054424 PACS number(s): 75.30.Gw

I. INTRODUCTION

The intermetallic compounds $R_2Co(Fe)_{17}$ (R denotes rare earth) have been the subject of intensive study during the last 30 years because of their outstanding magnetic characteristics and rich phenomenology, which are due to the coexistence of the complementary properties of $3d$ and $4f$ magnetism.[1] The peculiar properties of some Co-based compounds are exploited in the preparation of high-performance permanent magnets.[1,2] The possibility of improving the intrinsic magnetic properties (in particular, the magnetocrystalline anisotropy and the Curie temperature) by the insertion of relatively small amounts of nitrogen and carbon interstitial atoms[3] has renewed the technological interest towards the R_2Fe_{17} phases.

On the basis of their powder diffraction patterns, the 2:17 compounds are usually supposed to crystallize in the rhombohedral Th_2Zn_{17} crystal structure (when R=Pr,Nd,Sm) or in the hexagonal Th_2Ni_{17} structure (when R=Gd,Tb,Dy,Ho,Er,Tm,Lu). Both these structures can be thought as derived from the parent RM_5 hexagonal cell ($CaCu_5$) through the ordered replacement of 1/3 of the R atoms with the balance stoichiometric amount of metallic pairs M_2:

$$3(RM_5)+M_2 \rightarrow R_2M_{17}+R. \quad (1)$$

The rhombohedral Th_2Zn_{17} structure belongs to the space group $R\bar{3}m$, where a single site (6c) and four different sites (6c,9d,18f,18h, following the Wyckoff notation) are available for R and M atoms, respectively. In the hexagonal phase (space group $P63/mmm$) four sites ($4f$, $6g$, $12j$, $12k$) are still are occupied by M, while two sites ($2b$, $2c$) are available for R. The actual knowledge indicates that two metallic atoms are symmetrically positioned (in a dumbbell configuration) with respect to the basal plane of the structure containing the R atoms (Fig. 1). However, to the best of our knowledge, no accurate structure determination have been reported so far for R-M compounds.

In recent studies a double field-induced sharp transition was seen in the magnetization curve $M(H)$ of Pr_2Fe_{17} at two critical values of the applied magnetic field.[4,5] This peculiar feature has been interpreted[5] as the occurrence of a double first-order magnetization process (FOMP).[6] However, in the frame of the FOMP model, which considers the system as rigidly coupled and described by the anisotropy energy expression

$$E_A = K_1 \sin^2\theta + K_2 \sin^4\theta + \cdots, \quad (2)$$

the occurrence of a double transition in the $M(H)$ curves would require the use of an unrealistic eighth-order anisotropy constant. The attempt to describe the observed feature by using a two-sublattice model also failed.[5,7] In fact, even allowing for the occurrence of a canting angle[8] between the Pr and Fe sublattice magnetic moments during the magnetization process,[5] no satisfactory result was obtained when attributing only the second-order anisotropy constant to the Fe sublattice. Indeed Fe, in Y_2Fe_{17}, gives a planar anisotropy that is well described by only the K_1 anisotropy constant.[9]

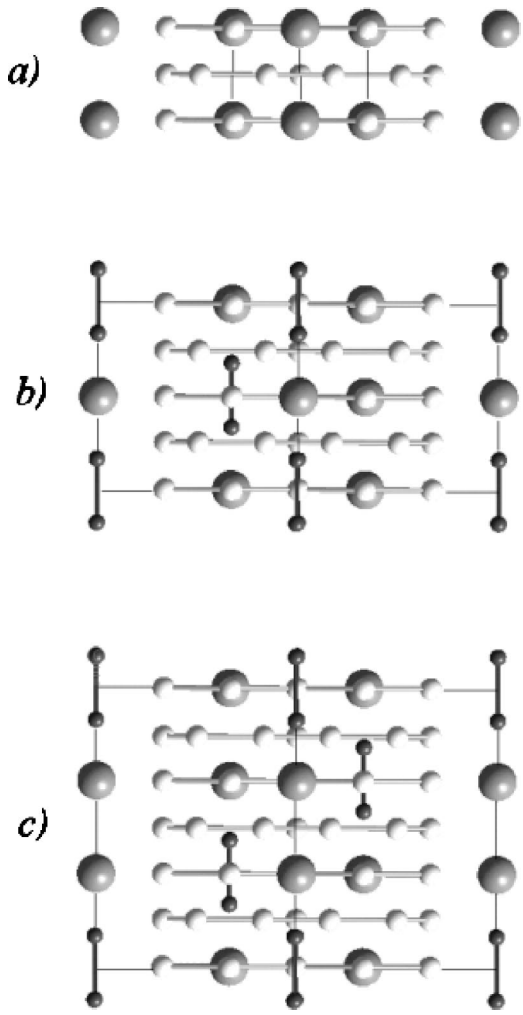

FIG. 1. Comparison of (a) the basic crystal structure of RM_5 with one of the (b) hexagonal and (c) rhombohedral R_2M_{17} phases, obtained by the ordered replacement of 1/3 of the R atoms with M_2 dumbbells.

In order to reproduce the observed double transition, it was found to be necessary that both sublattices be described by high-order (K_3) anisotropy constants. The Fe sublattice does not satisfy this last requirement. It was thus necessary to find the responsible second complex anisotropy contribution. The possibility for the samples to have off-stoichiometric composition (i.e., R in excess), the coexistence of mixed structures (hexagonal and rhombohedral), and the occurrence of extended volumetric defects were considered as possible sources of the required second contribution. A careful single-crystal x-ray diffraction analysis was thus undertaken in order to discover the possible presence of not yet reported deviations from the usually accepted Pr_2Fe_{17} structural model. The study was extended to the isostructural Pr_2Co_{17} compound. The magnetocrystalline anisotropy, as well as the Curie temperature (T_C) of compounds, which have been prepared with different starting compositions and thermal treatments, was measured along with x-ray diffraction.

II. EXPERIMENT

The polycrystalline samples were prepared by arc melting the required amount of pure elements (99.99%) under Ar atmosphere. In order to improve the sample homogeneity, the specimens were remelted three times and annealed. Nominal stoichiometric compositions and annealing parameters are reported in Table I. Suitable single crystals for the diffraction experiments were selected from crushed annealed polycrystalline materials. Single-crystal data were collected on both a Philips PW1100 and a Bruker AXS 100 CCD diffractometer at room temperature using Mo $K\alpha$ radiation. The structures were solved by direct methods using SIR97 (Ref. 10) and refined with SHELXL97 (Ref. 11).

The Curie temperature values were determined by thermomagnetic analysis (TMA), which consists of measuring the temperature dependence of the initial ac susceptibility (χ) in an applied field of about 4 Oe at 500 Hz. This technique was also used to check the sample single-phase character and homogeneity. This determination is straightforward with TMA, since multiple-phase behavior results in the presence of multiple $\chi(T)$ steps, while compositional inhomogeneities broaden the susceptibility drops.

The singular point detection[12] (SPD) technique was used to measure the temperature dependence of the anisotropy field H_A and the critical fields H_{cr} of magnetic-field- induced transitions. SPD allows for a precise determination of these quantities in polycrystalline samples.[12,13]

III. RESULTS AND DISCUSSION

A. Thermomagnetic analysis

From thermomagnetic analysis, all annealed samples resulted to be homogeneous. Pr-Fe samples were found to be single phase, while the presence of some amount of free Co was detected in Pr-Co specimens. An example of the $\chi(T)$ behavior in the two systems is shown in Fig. 2. All the measured T_C values are reported in Table I. For all the different Pr-Fe compounds the Curie temperature value was found to be the same within experimental error (285 ± 2 K). Due to the fact that the ordering temperature is driven by the $3d$-metal sublattice, this result indicates that all samples should contain the same amount of iron. In contrast, in the case of Pr-Co compounds, small but significant differences were observed between the T_C values of two groups of samples: those grown starting from the stoichiometric composition or with a Co excess and those with a Pr excess. This should correspond to different Co contents in the two groups.

B. Structural characterization

When a rhombohedral lattice is described in terms of an R-centered hexagonal cell, six sets of transformations can occur, three of them leading to the standard obverse setting and three related to the former by a simple inversion of the a and b axis, defining the reverse one. The two settings that imply the general reflection condition $-h+k+l=3n$ and $+h-k+l=3n$, respectively, are enanthiomorphic, so that the polarity is inverted moving from a set to the other. For

TABLE I. Nominal compositions, heat treatments, and some magnetic properties of Pr-Fe and Pr-Co samples.

Sample label	Composition	Heat treatment	T_C (K)	H_{cr1} (kOe) $T=105$ K	H_{cr2} (kOe) $T=105$ K	H_A (kOe) RT
F1	Pr_2Fe_{17}	1000 °C for 3 days +slow cooling	285	45.2±0.5	32.5±0.5	
F2	Pr_2Fe_{17}	1000 °C for 3 days +quenching	286	46.0±0.5	30.0±0.5	
F3	Pr_2Fe_{17} +10% Pr	1000 °C for 3 days +slow cooling		44.2±0.5	32.1±0.5	
F4	Pr_2Fe_{17} +10% Pr	1095 °C for 7 days +quenching	285	46.3±0.5	31.2±0.5	
F5	Pr_2Fe_{17} +15% Pr	1000 °C for 3 days +quenching	288	44.3±0.5	32.6±0.5	
C1	Pr_2Co_{17}	1000 °C for 3 days +quenching	1165			29.8±0.5
C2	Pr_2Co_{17} +10% Pr	1300 °C for 18 days +quenching	1158			20.5±0.5
C3	Pr_2Co_{17} +10% Pr	1200 °C for 8 days +quenching	1155			20.6±0.5
C4	Pr_2Co_{17} +25% Pr	1200 °C for 8 days +quenching	1155			18.1±0.5
C5	Pr_2Co_{17}	1200 °C for 8 days +quenching	1165			28.1±0.5

noncentrosymmetric space groups the true absolute configuration related to the obverse-reverse setting can be established only *a posteriori* on the basis of the refinement results.

Single-crystal diffraction experiments performed on several Pr_2Fe_{17} or Pr_2Co_{17} crystals, selected from different batches, pointed out for most samples the simultaneous presence of reflection classes obeying both general reflection conditions previously described. The phenomenon, not unusual in rhombohedral crystals, indicates the occurrence of reticular merohedry that can be interpreted in terms of the presence of obverse-reverse twinning domains within the same crystal. Therefore the data collection was performed in all cases in such a way as to access similar information for both domain types. The reflections were then grouped into three sets. The first one, consisting of the reflections with $l=3n$, is common to both twinning domains, whereas the other two, consisting of the $l\neq 3n$ reflections obeying the general condition $-h+k+l=3n$ and $+h-k+l=3n$, respectively, are representative of the diffraction contributions of the obverse and reverse twinning domains, respectively. In order to take into account the relative orientation of the two twinning domains within the same crystal, the original hkl indexes of the third reflections set where changed to $\bar{h}\,\bar{k}\,\bar{l}$ in order to transform the reverse lattice into an obverse one rotated by 180° with respect to the ab plane (i.e., in a further obverse lattice having the polar axis inverted with respect to original obverse lattice). This transformation allows the simultaneous refinement of the atomic parameters and of the diffraction contribution of the twinning domains, by using two different scale factors for the second and the third sets, whose sum was constrained to fit the scale factor of the common reflections set.

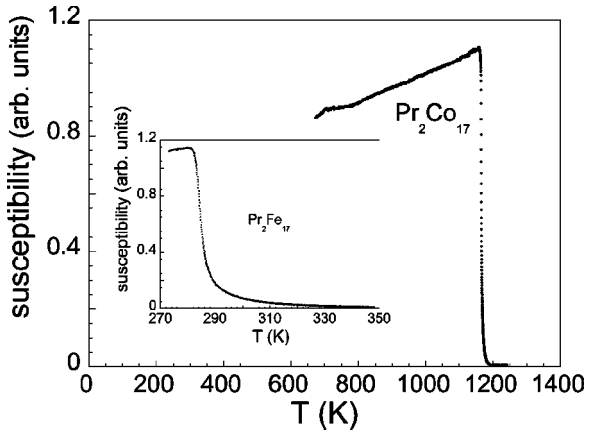

FIG. 2. Temperature dependence of the initial ac susceptibility $\chi(T)$ in Pr_2Co_{17} (sample C2). The $\chi(T)$ behavior for Pr_2Fe_{17} (sample F2) is shown in the inset.

The basic structure was solved by direct methods by using SIR97 on a single obverse set of reflections (i.e., the major twinning domain contribution) coupled with the common reflections set. Even in the presence of a significant contribution of the omitted second twinning domain to the intensities of the common reflections set, directs methods were able to find a solution compatible with the typical 2:17 rhombohedral arrangement by using the centrosymmetric $R\bar{3}m$ and the corresponding noncentrosymmetric $R3m$ space groups.

TABLE II. Lattice parameters, obverse/reverse volume fraction, and Pr excess for Pr-Fe and Pr-Co samples.

Sample	a (Å)	c (Å)	R (%)	Obverse/reverse volume fraction (%)	Pr excess (x)[a]
F1	8.578(1)	12.466(2)	5.4	72.8(1)/27.2(1)	
F2	8.594(1)	12.489(2)	8.0	not determined	
F3	8.577(1)	12.462(1)	5.1	78.4(1)/21.6(1)	
F4	8.569(1)	12.443(2)	5.0	75.8(1)/24.2(1)	
F5	8.592(1)	12.479(1)	10.2	83.0(2)/17.0(2)	
C1	8.443(1)	12.280(2)	4.4	92.4(1)/7.6(1)	1.0(3)
C2	8.454(1)	12.273(1)	6.4	61.5(1)/38.5(1)	5.7(3)
C3	8.455(1)	12.267(1)	8.5	61.9(1)/38.1(1)	4.5(4)
C4	8.450(2)	12.255(3)	3.4	100/0	5.0(3)
C5A[b]	8.457(1)	12.276(2)	7.1	96.6(1)/3.4(1)	2.3(4)
C5B[b]	8.434(1)	12.256(1)	7.9	83.4(2)/16.6(1)	0

[a]Pr excess refers to the substitution of cobalt dumbbells with Pr atoms, resulting in the chemical formula $Pr_{2+x}Co_{17-2x}$.
[b]The two samples are fragments of the C5 batch.

Preliminary refinement tests performed in both space groups showed similarities and discrepancies. The former are related to the appearance in the difference Fourier maps of residual peaks indicating a statistical distribution of Pr atoms and iron dumbbells in two of the three sites occupied by the rare-earth metal in the parent 1:5 structure. This feature is clearly related to the diffraction contribution of the neglected twinning domain, which is contained in the intensities of the common reflections set. The discrepancies consist mainly of the arrangement of the transition-metal layer at $z \simeq 1/6$, where each atom is univocally defined in the noncentrosymmetric space group, whereas it is statistically distributed over two positions in the centrosymmetric one. In this situation the ability to remove the disorder, in the absence of the inversion center, is solid evidence of a noncentrosymmetric structure. Therefore the final refinements were carried out in $R3m$ by using the complete diffraction data sets in order to refine the relative volumes of the twinning domains, as described previously.

1. Pr_2Fe_{17}

Several crystals from different batches have been investigated (Tables I and II). In spite of different starting compositions and annealing conditions, all the samples were found to be stoichiometric and quite similar from a structural point of view. Crystal data and refinement parameters for a typical Pr_2Fe_{17} crystal are reported in Table III. Atomic coordinates and displacement parameters are reported in Table IV and selected bond distances in Table V. The rhombohedral Pr_2Fe_{17} structure consists of alternate stacking along the c axis of two different layers resulting from different linking of Fe_6 hexagonal units (Fig. 3). One layer is a pure iron layer, while the second [the dark one in Fig. 3(a)] contains Pr atoms and iron dumbbells in the ratio 2:1. In the latter layer, the hindrance of the guests produces a deformation of the hexagonal units, which are enlarged around the Pr atom and contracted around the dumbbell.

The complete stacking sequence viewed along the c axis is shown in Fig. 3(b). The resulting structure is presented in Fig. 4. It can be seen that on one side the pure iron layers are far from planar, as a result of the deformation induced by the embedded iron dumbbells, whereas the Pr atoms are slightly displaced along the c axis with respect to the iron atoms of the same layer. These deformations are at the basis of the deviation of the structure from a centrosymmetrical model

TABLE III. Parameters for the x-ray diffraction of single crystals.

Sample label	F4	C4
Formula	Pr_2Fe_{17}	$Pr_{2.05}Co_{16.90}$
Lattice parameter a (Å)	8.569(1)	8.450(2)
Lattice parameter c (Å)	12.443(2)	12.255(3)
Space group	$R3m$	$R3m$
Cell volume (Å^3)	791.25(18)	756.0(3)
Calculated density (g cm^{-3})	7.752	8.467
Linear absorption coefficient (mm^{-1})	31.52	36.58
Diffractometer (Mo $K\alpha$)	Bruker SMART CCD	Philips PW1100
$2\theta_{max}$(deg)	49.0	76.1
Range	$-9 \leqslant h \leqslant 9$, $-8 \leqslant k \leqslant 8$, $-14 \leqslant l \leqslant 7$	$-14 \leqslant h \leqslant 14$, $-14 \leqslant k \leqslant 1$, $0 \leqslant l \leqslant 21$
Number of measured reflections	4243	8276
Number of unique reflections	1138[a]	549
Number of reflections with $F_o > 4\sigma(F_o)$	857	453
Number of refined parameters	41	43
R, wR2	0.050, 0.125	0.033, 0.060
Goodness of fit	0.862	0.911

[a]Not merged for compatibility with refinement of twined individuals, and corresponding to 455 really unique reflections.

TABLE IV. Atomic coordinates, occupancy factors (G) and equivalent isotropic displacement parameters for Pr_2M_{17} compounds.

Sample F4						
Atom	Wyckoff position	x	y	z	G(%)	$U_{eq}\times 10$(Å^2)
Pr1	3a	0	0	0.3521(3)	100	0.083(15)
Pr2	3a	0	0	0.6689(3)	100	0.109(16)
Fe1	3a	0	0	−0.0855(15)	100	0.070(43)
Fe2	3a	0	0	0.1043(8)	100	0.132(46)
Fe3	9b	−0.1673(12)	0.1673(12)	0.1795(15)	100	0.096(5)
Fe4	9b	0.5036(9)	0.4964(9)	0.1688(8)	100	0.097(25)
Fe5	9b	0.1653(8)	−0.1653(8)	0.1894(8)	100	0.104(25)
Fe6	18c	0.2881(10)	0.2868(10)	0.0111(10)	100	0.122(5)

Sample C4						
Atom	Wyckoff position	x	y	z	G(%)	U_{eq} or $U_{iso}\times 10$ (Å^2)
Pr1	3a	0	0	0.3525(2)	100	0.048(8)
Pr2	3a	0	0	0.6641(2)	100	0.038(8)
Pr3	3a	0	0	0.0006(23)	5.0(3)	0.04
Co1	3a	0	0	−0.0878(8)	95.0(3)	0.042(21)
Co2	3a	0	0	0.1047(9)	95.0(3)	0.035(22)
Co3	9b	−0.1659(7)	0.1659(7)	0.1747(8)	100	0.030(2)
Co4	9b	0.5032(5)	0.4968(5)	0.1626(5)	100	0.022(15)
Co5	9b	0.1645(5)	−0.1645(5)	0.1873(5)	100	0.056(15)
Co6A	18c	0.2873(5)	0.2856(5)	0.0087(6)	95.0(3)	0.037(8)
Co6B	18c	0.3333	0.3333	−0.0010(27)	5.0(3)	0.04

and they have not been seen in previous studies of this structure type. The absence of the center of symmetry in the $R3m$ space group results in two crystallographically independent Pr sites. Despite the fact that they differ in position with respect to the basal R-M plane, it is found that these two sites maintain a quite similar environment in the structure, since the average Pr-Fe distance is almost equivalent [3.172(10) and 3.158(11) Å for Pr1 and Pr2, respectively].

Another interesting result arose from the refinement of the twinning domain contribution to the diffraction of the crystals. As can be seen from Table II, the refined volume fraction of the two twinning domains is quite independent of the measured sample. This phenomenon can be understood only by supposing the obverse-reverse twinning, resulting in the inversion of the polar axis, as a very frequent stacking fault that characterizes this phase. Only under these conditions can the probability to have almost equivalent twinning volume fractions by choosing different fragments in the same or in different batches become realistic.

2. Pr_2Co_{17}

As in case of the iron compounds, several crystal fragments coming from different batches have been investigated (Table I). Differently from the iron case, all the analyzed samples were found to be nonstoichiometric, with a Pr excess up to 6% of the nominal rare-earth content of the 2:17 composition. The praseodymium excess in the 2:17 phase seems to be influenced by the starting stoichiometry, being typically $\simeq 1\%$ in nominally stoichiometric or cobalt-rich samples and larger ($\simeq 5\%$) in presence of a rare-earth excess in the starting mixture. A unique stoichiometric crystal (C5B) was found in a batch prepared starting with Co excess (nominally Pr_2Co_{18}), but other crystals of the same batch were found to be nonstoichiometric (e.g., with a Pr excess larger than 2% in C5A). This seems to indicate a possible effect of the nonstoichiometry on the stabilization of the cobalt-based phase. On the other side, the Pr excess shows an upper limit at about 6%, which cannot be increased further by increasing the Pr content in the starting mixture. On the basis of these results the analyzed samples can be grouped in two broad sets, corresponding to a Pr excess ranging around 1% and 5%, which are obtained when starting from stoichiometric composition (and Co excess) and with Pr excess, respectively.

Structural analysis showed that the general features of the structure are the same found for the corresponding iron compound. The main difference consisted in a residual electron density peak located between the two Co atoms forming the dumbbell, which has been interpreted in terms of a partial substitution of the Co dumbbell with a Pr atom in the ratio 1:1, leading to a chemical formula $Pr_{2+x}Co_{17-2x}$. This hypothesis was confirmed by the structural refinement, leading to the appearance of a second residual peak located near the Co6A position. Refining this peak as a partially occupied Co6B site, alternative to the Co6A position, its occupancy converged to a value close to that of the additional Pr atoms

TABLE V. Selected interatomic distances (Å) for Pr_2M_{17} compounds.

Sample F4			Sample C4		
Pr1	−Pr2	3.892(6)	Pr1	−Pr2	3.810(4)
	−Fe2	3.110(18)		−Co2	3.029(11)
	−3 Fe3	3.316(14)		−3 Co3	3.258(9)
	−3 Fe4	3.113(8)		−3 Co4	3.042(6)
	−3 Fe5	3.243(8)		−3 Co5	3.214(6)
	−3 Fe5	3.213(8)		−3 Co5	3.142(6)
	−6 Fe6	3.083(9)		−6 Co6A	3.047(5)
				−6 Co6B	2.827(3)
Pr2	−Fe1	3.056(19)	Pr2	−Co1	3.032(10)
	−3 Fe3	3.307(15)		−3 Co3	3.272(9)
	−3 Fe4	3.270(10)		−3 Co4	3.226(5)
	−3 Fe4	3.186(10)		−3 Co4	3.131(6)
	−3 Fe5	3.086(8)		−3 Co5	3.030(5)
	−6 Fe6	3.066(9)		−6 Co6A	3.027(5)
				−6 Co6B	2.817(1)
			Pr3	−3 Co3	3.23(2)
				−3 Co3	3.129(19)
				−3 Co4	3.180(19)
				−3 Co5	3.32(2)
				−6 Co6B	2.817(1)
Fe1	−Fe2	2.39(3)	Co1	−Co2	2.354(15)
	−3 Fe3	2.607(12)		−3 Co3	2.599(7)
	−3 Fe4	2.612(12)		−3 Co4	2.598(7)
	−6 Fe6	2.741(13)		−6 Co6A	2.693(7)
Fe2	−3 Fe3	2.645(12)	Co2	−3 Co3	2.575(7)
	−3 Fe5	2.664(10)		−3 Co5	2.611(6)
	−6 Fe6	2.733(13)		−6 Co6A	2.690(7)
Fe3	−2 Fe4	2.446(11)	Co3	−2 Co4	2.427(6)
	−2 Fe5	2.471(11)		−2 Co5	2.423(6)
	−2 Fe6	2.451(20)		−2 Co6A	2.409(11)
	−2 Fe6	2.421(20)		−2 Co6A	2.380(11)
				−2 Co6B	2.57(3)
				−2 Co6B	2.39(3)
Fe4	−2 Fe5	2.524(9)	Co4	−2 Co5	2.497(6)
	−2 Fe6	2.520(14)		−2 Co6A	2.517(9)
	−2 Fe6	2.678(13)		−2 Co6A	2.607(8)
				−2 Co6B	2.51(3)
				−2 Co6B	2.45(3)
Fe5	−2 Fe6	2.653(12)	Co5	−2 Co6A	2.615(8)
	−2 Fe6	2.563(14)		−2 Co6A	2.522(9)
				−2 Co6B	2.70(3)
				−2 Co6B	2.26(3)
Fe6	−Fe6 [a]	2.480(13)	Co6A	−Co6A[a]	2.442(7)
	−Fe6 [b]	2.447(13)		−Co6A[b]	2.399(7)
	−Fe6 [c]	3.462(8)		−Co6A[c]	3.609(4)
				−Co6B[a,b,c]	2.817(7)

[a]Relates to a transformation $-x+y,y,z$.
[b]Relates to a transformation $x,x-y,z$.
[c]Relates to a transformation $x,x-y,z$.

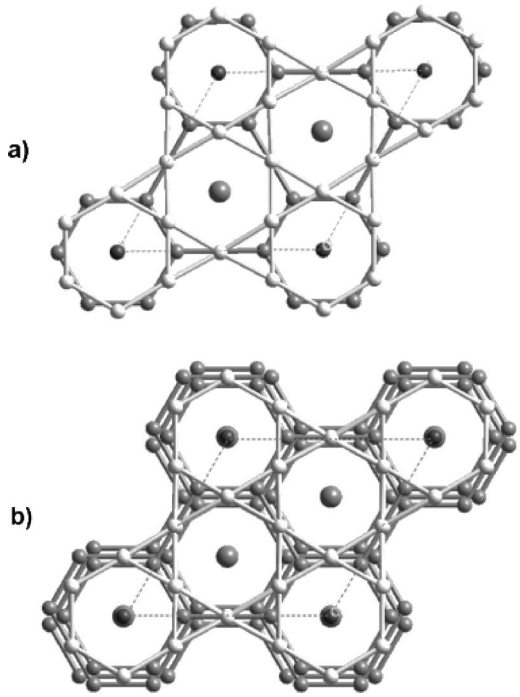

FIG. 3. Projection along the *c* axis of the Pr_2Fe_{17} structure, which consists of the alternate stacking of pure iron layers (light gray) and mixed layers (midgray) containing Pr atoms (large balls) and iron dumbbells (dark gray) in the ratio 2/1: (a) superposition of a couple of layers; (b) superposition of the different layers in the whole structure.

(Pr3), suggesting the existence of a strong relationship between the two residual peaks. As shown in Fig. 5, the substitution of a Co dumbbell by a Pr atom results in a modification of the corresponding Co layer. The hexagonal network formed by Co6A atoms, which is distorted in the stoichiometric 2:17 phase by the hindrance of Pr atoms and Co

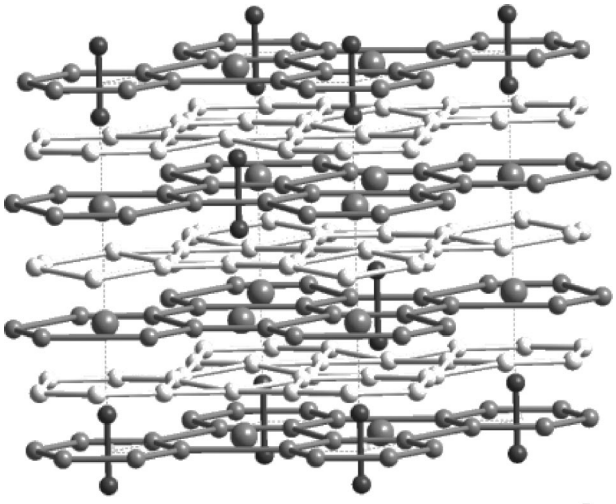

FIG. 4. A view of the Pr_2Fe_{17} structure showing the puckering of iron layers (light gray). Large balls represent Pr atoms, whereas iron dumbbells are shown in dark gray.

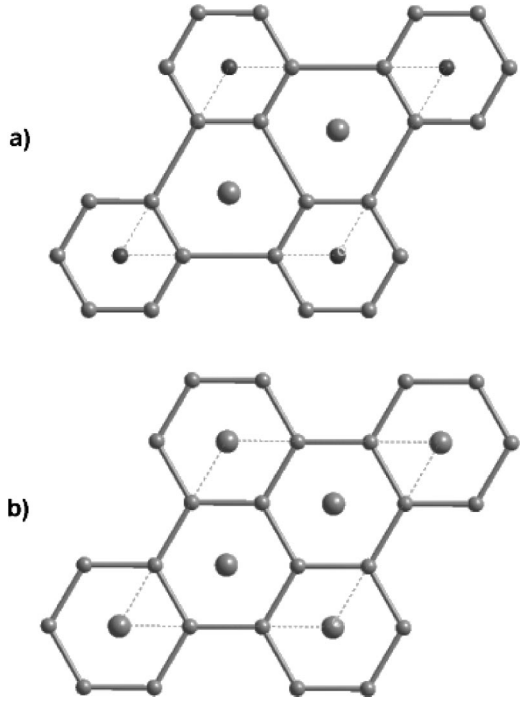

FIG. 5. The modification of the Co arrangement in the mixed Pr-Co planes of the ideal Pr_2Co_{17} structure (a) with the substitution of Co dumbbells by Pr atoms (b) that restore the typical situation of the $PrCo_5$ structure.

dumbbells [Fig. 5(a)], becomes regular by considering the displaced Co6B position, as required by the insertion of the substitutional Pr atom for dumbbells. Such a substitution transforms the layer in a way that is typically observed for the 1:5 phase [Fig. 5(b)]. As a consequence of the final refinement the site occupancy of Co6B was constrained to that of Pr3 and the *x* and *y* coordinates for the same atom were fixed to the values found in the difference Fourier maps (1/3, 1/3), because of the proximity of the almost fully occupied Co6A site.

Crystal data and refinement parameters for a typical $Pr_{2+x}Co_{17-2x}$ crystal showing a large Pr excess are reported in Table III. Atomic coordinates and displacement parameters are reported in Table IV and selected bond distances in Table V. As in the case of the Pr-Fe system the pure $3d$-metal layer shows a puckered arrangement and the two independent Pr atoms are displaced along the *c* axis with respect to the Co atoms forming the mixed Pr-Co layer. The average Pr-Co distance involving the two independent Pr sites is equivalent within the error (σ) [3.120(6) and 3.114(6) Å for Pr1 and Pr2, respectively].

From the results of the structural analysis of the Pr-Co system, the 2:17 structure seems to be stabilized by the presence of excess Pr. This can be interpreted in terms of stacking faults of the corresponding 1:5 parent phase, whose presence in the Pr-Co system is well known. In contrast, the 2:17 structure in the Pr-Fe system, for which the formation of the 1:5 phase has not been reported, seems to be stabilized by a different mechanism, consisting of a frequent inversion of the polar axis, as revealed by a systematic obverse-reverse

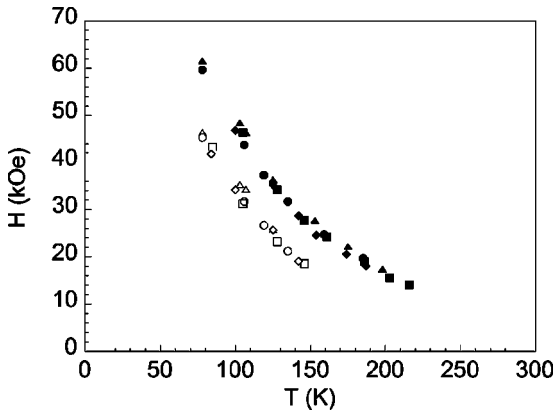

FIG. 6. Temperature dependence of the critical field values H_{cr1} (filled symbols) and H_{cr2} (open symbols) of the magnetic-field-induced FOMPs in the samples F1, F2, F3, and F4 of composition Pr_2Fe_{17}.

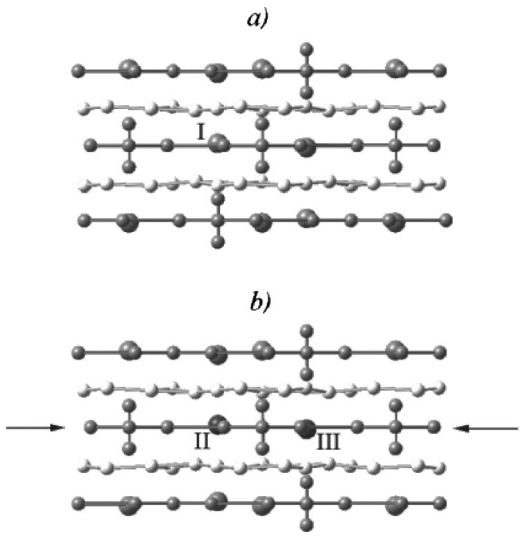

FIG. 7. Generation of nonequivalent Pr sites at the twin boundary of obverse-reverse domains: (a) a twin-free structure where all the Pr atoms have a similar environment (denoted by I); (b) a twinned structure, where nonequivalent sites (II and III) are produced in the twin plane (indicated by arrows).

twinning, which affects, to a similar extent, all the examined crystals. This obverse-reverse twinning has also been found in most of the cobalt phase crystals (Table II), but differently from the iron case, the relative twinning volume fraction, refined on the basis of the diffraction data, differs from sample to sample even within the same batch. The occurrence of twinning seems to be dependent on the considered sample (or part of the sample), while no relation was found with the starting composition as well as with the different annealing conditions. This leads to the conclusion that the polar obverse-reverse twinning in Pr-Co represents a stacking fault that has to be considered to be casual rather than systematic, so that twinned or untwinned fragments could be randomly found in the same batch.

C. Magnetic measurements

It is known that in Pr_2Fe_{17} the easy magnetization direction is in the basal plane of the rhombohedral structure and that a double FOMP transition occurs at low temperatures for critical values (H_{cr}) of the magnetic field applied along the hard *c* axis.[4,5] Using the SPD technique the H_{cr} measurement has been performed, as a function of temperature, on the actual series of Pr-Fe samples (Table I). As seen in Fig. 6, no differences can be found (within the experimental error) among the critical field values (H_{cr}) for the different samples in the considered temperature range. This result is consistent with the x-ray diffraction determinations, which show that all Pr_2Fe_{17} samples have the same stoichiometric composition, irrespective of the nominal Pr/Fe ratio and annealing conditions. This conclusion is also supported by the results of TMA, which indicate the occurrence of the same T_C value for all the Pr-Fe compounds. On the other hand, the peculiarity of magnetization curves of Pr_2Fe_{17}, which contains two field-induced transitions (FOMP), was explained[7] only if at least two different Pr contributions to the anisotropy were taken into account; this is not the case when considering the usual centrosymmetric $R\bar{3}m$ structure. The two crystallographic inequivalent Pr1 and Pr2 sites, occurring in the noncentrosymmetric $R3m$ structure, could also be magnetically different, thus supplying opposite contributions to the anisotropy. It must be considered that these two independent atoms have quite a similar environment in a defect-free rhombohedral structure (they are bonded to only one iron atom of a dumbbell belonging to an adjacent layer; see site I in Fig. 7). However, recent density functional calculations[14] have shown that slightly different positions and charge distributions of Fe and Co atoms in intermetallic compounds may give rise to a change of sign for the leading crystal-field parameter B_2^0, hence to opposite second-order anisotropy contributions. As a simple test, we performed crystal-field evaluations using the coordinates given in Table IV, with the effective ionic charges Q_ℓ^{eff} calculated for R_2Fe_{17} compounds.[15] The values of the leading crystal-field parameter

$$B_2^0 = -\sum_\ell \frac{eQ_\ell^{\text{eff}}}{8\pi\epsilon_0 R_\ell^3}(3\cos^2\Theta_\ell - 1) \qquad (3)$$

are not significantly different for the two Pr ions. It is therefore unlikely that the two Pr1 and Pr2 sites are actually magnetically inequivalent.

On the other hand, if the real structure is taken into account instead of the ideal defect-free structure, it is found that Pr atoms lying in a twinning plane would have necessarily a modified Fe environment with respect to a twinning-free situation. In particular, one Pr atom would be bonded to an additional iron atom of a dumbbell, whereas the second

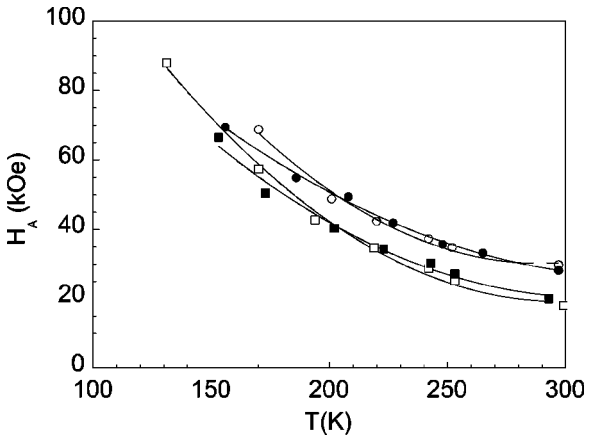

FIG. 8. Temperature dependence of the anisotropy field value (H_A) for the samples C1 (empty dots), C2-C3 (filled squares), C4 (empty squares), C5 (filled dots).

would interact with no dumbbell atoms at all (sites II and IIIin Fig. 7). These two sites are magnetically nonequivalent to the usual rare-earth sites. Since the occurrence of the polar twinning has to be considered systematic and very frequent in Pr_2Fe_{17} (for the previously discussed reasons), these two additional sites will contribute significantly to the global magnetic properties of the Pr_2Fe_{17} phase, and they can be considered as the source of the magnetic competition that creates the magnetic transitions in the $M(H)$ curve of Pr_2Fe_{17}.

Concerning Pr_2Co_{17}, it is known that the easy magnetization direction is along the c axis of the rhombohedral structure in the whole ferromagnetic range. X-ray diffraction experiments show that this system, in spite of the starting composition, usually contains some Pr excess. On the basis of the structural analysis, the samples can be grouped in two broad sets, corresponding to a Pr excess ranging around 1% and 5%, that are, respectively, obtained when starting from a stoichiometric composition (and Co excess) and with Pr excess. Consistently with this finding, the measure of the anisotropy field (H_A), performed by the SPD technique, shows the occurrence of two groups of H_A values that differ by more than 30% at room temperature (RT) (Fig. 8). The small constitutional differences existing within the two groups of samples reflects the differences in H_A that are observed at low temperatures.

IV. CONCLUSIONS

Novel structural features have been seen in the Pr_2Fe_{17} and Pr_2Co_{17} rhombohedral intermetallic compounds. Some of these features are common characteristics of the two compounds, while others appear to be specific to the cobalt- or iron-based phase. In particular, the common characteristics are as follows.

(1) The $3d$ atoms have a puckered arrangement in the $3d$-metal plane of the rhombohedral structure. This arrangement is a direct consequence of the presence in the structure of the out-of-plane $3d$ atoms, which correspond to the dumbbell sites.

(2) The Pr atoms do not lie in the Pr-M basal plane. They are displaced (above and below) with respect to the plane, moving along c in the opposite direction with respect to the short apical interaction with the M atom of a dumbbell.

(3) As a consequence of the puckered structure, the 2:17 rhombohedral phase must be described in the noncentrosimmetric $R3m$ space group rather than in the usual centrosymmetric $R\bar{3}m$ one. This change in the local symmetry could have an effect on the microscopic description of the planar component of the magnetocrystalline anisotropy.

In the case of Pr-Fe compounds it has been found that the resultant phases always have stoichiometric composition, even in presence of a nominal excess (from 0 to 25%) of Pr with respect to the stoichiometric composition. In contrast, in the case of Co, the compounds are usually found to be nonstoichiometric, with some Pr excess. However, two groups of samples were identified: samples with low Pr excess ($\simeq 1\%$) were always obtained when melting elements in the nominal composition or with an excess of cobalt, while melting with a Pr excess, an amount of Pr of about 5% ($Pr_{2+x}Co_{17-2x}$) with respect to the stoichiometric composition was found. The quantity x increases with Pr excess up to the maximum value of 6%.

The different compositional behavior of Co and Fe compounds seems to be correlated to the existence of the parent RCo_5 phase, for which the possibility of changing its compositional ratio from 1:5 to 2:17 continuously was also shown.[16] As a consequence, in the case of Pr_2Co_{17}, an excess of R can be accommodated, with a resulting compositional shift toward the 1:5 stoichiometric composition. The occurrence of Pr excess even when melting a mixture of elements with Co excess indicate a possible effect of nonstoichiometry on the stabilization of the cobalt-based phase. In contrast, the 1:5 phase is not formed in the R-Fe system,[17–19] and as a consequence, the stoichiometric shift from 2:17 to 1:5 should not take place in the case of Fe. In Pr_2Fe_{17}, a stabilizing role seems to be played by the frequent occurrence of the polarity inversion of the rhombohedral axis (obverse-reverse transition).

It can be inferred that in the mixed R-(Fe,Co) system, the strong preference of Fe for the dumbbell sites should prevent the Pr replacement for Fe in these sites. This should inhibit the occurrence of Pr excess, thus favoring a Pr-Fe-like behavior. As for the replacement of Pr atoms by cobalt dumbbells, it has not been possible to establish if it takes place randomly or rather concentrates in specific planes.

The presence of a polarity inversion gives rise to multiple Pr magnetic sites and thus to different contributions to the magnetocrystalline anisotropy. The peculiar magnetization curves of Pr_2Fe_{17}, which contain two field-induced transitions (FOMP), that occur at two different critical values of the applied magnetic field, were indeed explained[7] only if two opposite Pr contributions to the anisotropy were taken into account. The presence of independent Pr sites, which has been found in this study, can be the source of the second required contribution.

[1] J.J.M. Franse and R. Radwanski, in *Handbook of Magnetic Materials*, edited by K.H.J Buschow (Elsevier Science, Amsterdam, 1993), Vol. 7.
[2] K.J. Strnat, in *Handbook of Magnetic Materials*, edited by E.P. Wohfarth and K.H.J Buschow (Elsevier Science, Amsterdam, 1988), Vol. 4.
[3] H. Fuji and H. Sun, in *Handbook of Magnetic Materials*, edited by K.H.J Buschow (Elsevier Science, Amsterdam, 1995), Vol. 9.
[4] X.C. Kou, F.R. de Boer, R. Grossinger, G. Wiesinger, H. Suzuki, H. Kitazawa, T. Takamasu, and G. Kido, J. Magn. Magn. Mater. **177-181**, 1002 (1998).
[5] F. Albertini, F. Bolzoni, A. Paoluzi, L. Pareti, and E. Zannoni, Physica B **294-295**, 172 (2001).
[6] G. Asti and F. Bolzoni, J. Magn. Magn. Mater. **20**, 29 (1980).
[7] A. Paoluzi, L. Pareti, F. Bolzoni, E. Zannoni, N. Magnani, J. Magn. Magn. Mater. **242-245**, 1362 (2002).
[8] S. Rinaldi and L. Pareti, J. Appl. Phys. **50**, 7719 (1979).
[9] B. Matthaey, J.J.M. Franse, S. Sinnema, and R. Radwanski, J. Phys. (Paris), Colloq. **49(C8)**, 533 (1988).
[10] A. Altomare, M.C. Burla, M. Camalli, G. Cascarano, C. Giacovazzo, A. Guagliardi, A.G.G. Moliterni, G. Polidori, and R. Spagna, J. Appl. Crystallogr. **32**, 115 (1999).
[11] G.M. Sheldrick, *SHELXL97, Program for Crystal Structure Refinement* (University of Göttingen, Germany, 1997).
[12] G. Asti and S. Rinaldi, J. Appl. Phys. **45**, 3600 (1974).
[13] L. Pareti, A. Paoluzi, and N. Magnani, J. Magn. Magn. Mater. **251**, 178 (2002).
[14] M.D. Kuzmin, M. Richter, and K.H.J. Buschow, Solid State Commun. **113**, 47 (2000).
[15] Z. Zeng, Q.Q. Zheng, and W.Y. Lai, Phys. Rev. B **49**, 6741 (1994).
[16] L. Pareti, M. Solzi, and G. Marusi, J. Appl. Phys. **72**, 3009 (1992).
[17] K.H.J. Buschow, Rep. Prog. Phys. **40**, 1179 (1977).
[18] A.R. Miedema, R. Boom, and F.R. de Boer, J. Less-Common Met. **41**, 283 (1975).
[19] H.R. Kirchmayr and C. A. Poldy, in *Handbook on the Physics and Chemistry of Rare Earths*, edited by K.A. Gschneider Jr. and L. Eyring (North Holland, Amsterdam, 1979), Vol. 2.